Proceedings of the 7th International Conference on Mechanics and Materials in Design
Albufeira/Portugal 11-15 June 2017. Editors J.F. Silva Gomes and S.A. Meguid.
Publ. INEGI/FEUP (2017)

PAPER REF: 6975

HIGH-SPEED DEFORMATION AND DESTRUCTION OF CONCRETE AND BRICK

Anatoly Bragov[1(*)], Bhushan Karihaloo[2], Aleksandr Konstantinov[1], Leopold Kruszka[3], Dmitriy Lamzin[1], Andrey Lomunov[1], Yury Petrov[4]

[1]Research Institute of Mechanical, Lobachevsky State University, Nizhny Novgorod, Russia
[2]School of Engineering, Cardiff University, Cardiff, UK
[3]Faculty of Civil Engineering and Geodesy, Military University of Technology, Warsaw, Poland
[4]Saint Petersburg State University, Saint Petersburg, Russia
[(*)]*Email:* bragov@mech.unn.ru

ABSTRACT

The results of dynamic tests of ceramic brick, as well as fine-grained concrete and fiber-reinforced concrete are reported. In addition to compression tests, the modifications of Kolsky method are used to determine the dynamic properties in tension and shear. For fiber-reinforced concrete the dynamic fracture toughness is measured on three-point bending beams with a U-shaped notch. Stress-strain curves are constructed under different regimes of dynamic impact. Strength, deformation, timing and energy characteristics are obtained, as well as their dependence on strain rate, stress growth rate and load amplitude. The effect of the strain rate, the rate of stress growth, and the type of stress state on the properties of the tested materials is noted. For a theoretical description of the dynamic strength dependency, the theory of incubation time is used. The inclusion of an additional measured characteristic of strength (i.e., the incubation time) and the known quasi-static strength parameter (i.e., the limit stress) makes it possible to construct the dependences of the maximum crushing stress on the rate of loading (deformation) without having to perform numerous experiments for any type and character of the load.

Keywords: concrete, fiber-reinforced concrete, brick, dynamic strength, splitting.

INTRODUCTION

Due to unexpected events, such as a terror attack, technological catastrophes, accompanied by intense shocking or explosion actions, that cannot be anticipated at the stage of design of residential buildings, industrial facilities, nuclear facilities it becomes imperative to know how the building materials such as concrete, bricks will behave under such dynamic loads.

This work is devoted to research of static and dynamic properties of typical building materials, which are brittle in nature: a fine-grained concrete, fiber-reinforced concrete and ceramic brick. These materials are widely used in the protective and supporting structures of different categories of structures. Compared to conventional concrete, fiber-concrete has higher static compressive, tensile and shear strengths, impact and fatigue strength, fracture toughness, and resistance to frost, water penetration, heat and fire.

EXPERIMENTAL METHODS

Dynamic tests were carried out by the known Kolsky method using split Hopkinson pressure bar (SHPB) of different configurations (Fig.1). In addition to compression tests, the

modifications of Kolsky method were used to determine the dynamic properties in tension (Brazilian test) and shear.

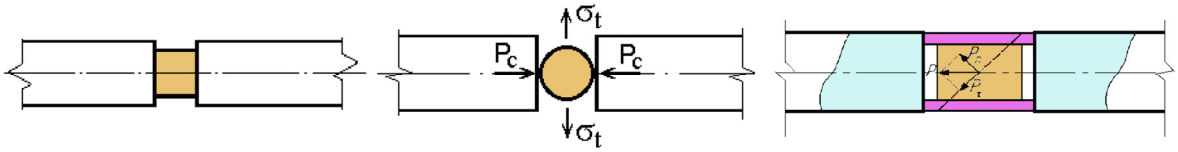

Fig. 1 - Types of testing based on the Kolsky method

It should be noted that in order to determine the shear strength the original modification of the SHPB first proposed by the authors (Bragov et al., 2017) is used. To determine the dynamic shear strength, a specimen (denoted 5 in Fig. 2) from the material to be examined is located in a rigid (steel) casing 3 and 4, cut at an angle α to the horizontal.

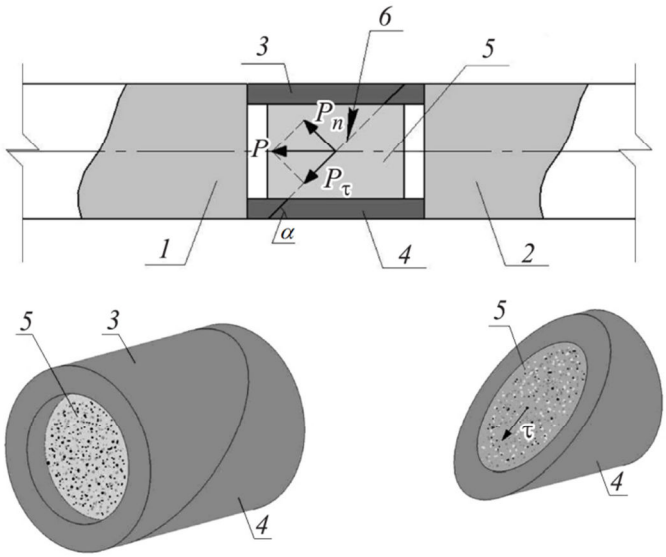

Fig. 2 - Shear test scheme: 1 - incident bar, 2 - transmitter bar, 3, 4 - parts of the split casing, 5 - sample, 6 - shear plane

In order for the specimen to undergo only shear without compression, its length must be less than the length of the cut tube casing. The cage with the specimen is placed between the measuring bars: the incident bar 1 and the transmitter bar 2. Since the yield strength of the cage is at least an order of magnitude greater than the strength of the tested specimen, the cage can be regarded as non-deformable. The compression pulse in the loading bar causes a small displacement of the two parts of the split casing along the plane of the cut 6, which leads to deformation and fracture of the brittle specimen.

Using the strain pulse $\varepsilon^T(t)$ recorded in the transmitted bar, it is possible to obtain the time dependence of the shear stress in the specimen:

$$\tau(t) = \frac{EA\cos\alpha\sin\alpha}{\pi R^2}\cdot\varepsilon^T(t).$$

A relative displacement of the points of the sample along the inclined plane of shear based on the strain pulses registered in the measuring bars can be expressed by the formula:

$$\varepsilon_\tau(t) = \frac{Ctg\alpha}{2R}\int_0^t\left(\varepsilon^I(t)-\varepsilon^R(t)-\varepsilon^T(t)\right)\cdot dt$$

where R is the inner radius of the cage, and E and A are the Young's modulus and the cross-sectional area of the transmitter bar, respectively.

The dynamic fracture toughness of the fiber-reinforced concrete was measured on three-point bending beams with a U-shaped notch. The specimen in this case is located between the ends of three measuring bars: the incident bar and two transmitter bars (Figure 3).

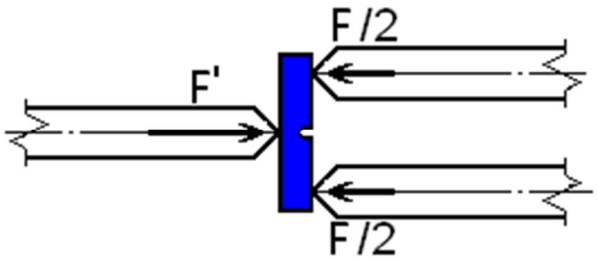

Fig. 3 - Scheme of the loading of a beam specimen during a fracture impact tougness test

During the test, the incident $\varepsilon^I(t)$ and reflected $\varepsilon^R(t)$ pulses in the incident bar are recorded, as well as the two pulses $\varepsilon_1^T(t)$ and $\varepsilon_2^T(t)$ transmitted through the specimen in the two transmitter bars. The beam deflection $l(t)$ and the force $F(t)$ acting on the specimen during loading are determined by processing these pulses. After synchronization of the obtained dependencies, a graph $F(l)$ is constructed and the energy (impact work) needed to fail the material is determined:

$$KU = \int_0^l F(l) \cdot dl \,.$$

The fracture toughness KCU is defined as the ratio of the impact work KU to the net initial cross-sectional area of the specimen at the notched section (at the stress concentration site):

$$KCU = \frac{KU}{BH_1},$$

where B and H_1 are the width and net height of the cross section of the beam specimen at the stress concentration site.

For a theoretical description of the dynamic dependencies, the theory of the incubation time of failure was used (Petrov, Utkin, 1989; Petrov, Morozov, 1996; Bragov, Petrov, Karihaloo et al, 2015). Sudden deformation depends on the amplitude and speed of application of the impact load. The reaction of the material to these energy input characteristics depends on the chosen failure criterion. The incubation time τ characterizes the sensitivity of the material to the rate of application of the load at a given point (or to the rate of deformation) that causes failure.

In particular cases of dynamic failure, the criterion of incubation time has the form:

- compression failure

$$\frac{1}{\tau}\int_{t-\tau}^{t} \sigma(t')dt' \le \sigma_{cr}^{comp},$$

where $\sigma(t)$ is the dependence of the average compressive stress in the specimen on time, σ_{cr}^{comp} - static compressive strength.

- tensile failure

$$\frac{1}{\tau}\int_{t-\tau}^{t}\sigma(t')dt' \le \sigma_{cr}^{tens},$$

where $\sigma(t)$ is the dependence of the tensile stress at the center of the sample on time, σ_{cr}^{tens} - static tensile strength.

- Complete failure of three-point bending of beam with a notch

$$\frac{1}{\tau}\int_{t-\tau}^{t}W(t')dt' \le W_c,$$

where $W(t)$ is the time profile of the work spent per unit of the cross section of the sample, W_c is the specific work expended on fracture under quasi-static loading.

TEST SPECIMENS

For compression test, cylindrical specimens (length 10 mm, diameter 18 mm) were made from ceramic bricks of the class designation 150. For the splitting test, the specimens had a diameter of 18 mm and length 20 mm.

The mechanical properties of fine-grained concrete M25 were studied in dry and water-saturated states. The mix used cement grade 43, sand with grain size 2, as well as super-plasticizer Muraplast FK-63 and stabilizer Reostab. The density of the samples was 2000 kg/m^3 in the dry and 2100 kg/m^3 in the water-saturated state. The specimens were cylindrical with a diameter of 20 mm and a length of 10 mm or 20 mm for both static and dynamic tests in compression and splitting.

Dynamic properties of the advanced fiber-reinforced concrete CARDIFRC (Alaee and Karihaloo, 2003), developed and manufactured at the University of Cardiff, UK were also investigated. This fiber-reinforced concrete has a fine-grained structure and contains brass-coated thin steel fibers (diameter 0.15 mm, length 6 or 13 mm). Specimens for compression and splitting tests were in the form of cylinders with a diameter of ~15 mm and a height of ~10 mm. Dynamic experiments on three-point bend beams with a U-shaped notch were made on installations with a diameter of measuring bars of 20 mm and 60 mm to determine the dynamic toughness of this fiber-reinforced concrete. For tests on the SHPB-20 installation, the beams had the following geometric dimensions: L≈66 mm, H≈20 mm, B≈11 mm, H_1≈15 mm. For tests on the SHPB-60 installation, the geometrical dimensions of the beams were as follows: L≈200 mm, H≈81 mm, B≈43 mm, H_1≈61 mm.

RESULTS AND DISCUSSION

As a result of the dynamic tests the dynamic stress-strain curves were obtained for the above materials under compression. By varying the speed of striker, loading regimes were achieved in which the specimen either retained apparent integrity, or had cracks on the surface or some internal damage, or was fractured completely into large or small pieces. Besides the dynamic compressive strength, the limiting values of the ultimate strength have also been determined in splitting and shear.

Figure 3 shows the average stress-strain curves of ceramic bricks with the history of strain rate variation obtained under different dynamic loading regimes. The solid lines show the

dependences σ~ε (the left vertical axis is stress), and the dotted lines of the corresponding color are the dependences $\dot{\varepsilon}$ ~ε (the right vertical axis is the strain rate).

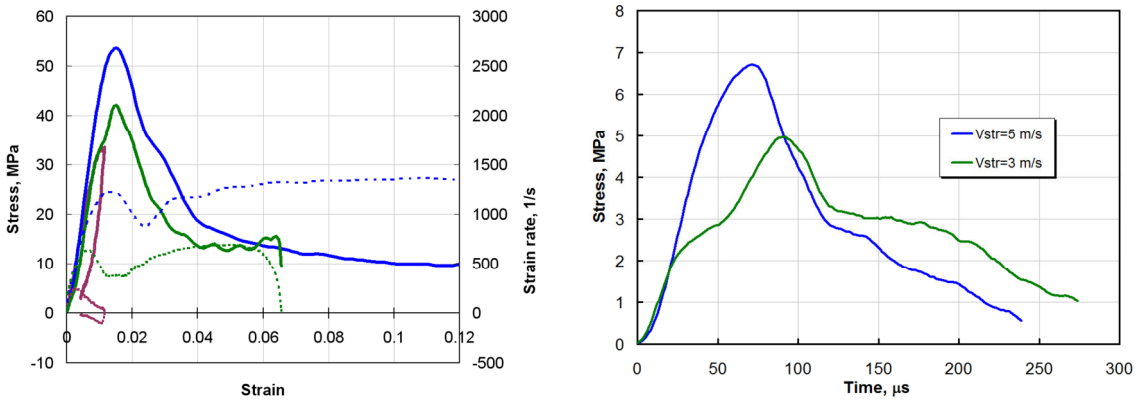

(a) (b)

Fig. 3 - Mechanical properties of ceramic brick in compression (a) and splitting (b)

In these plots, it is evident that the initial part of the loading branch (stress-strain curve) is nearly linear. The slope of the loading branch in this region of the curves is practically the same for different strain rates. During deformation, after the stress in the sample reaches a limiting value, the tested material begins to crumble rapidly, and the formation of micro- and macro-cracks leads to a decrease in the stress level with increasing deformation. The curves characterizing the process of failure can have a fairly long tail segment.

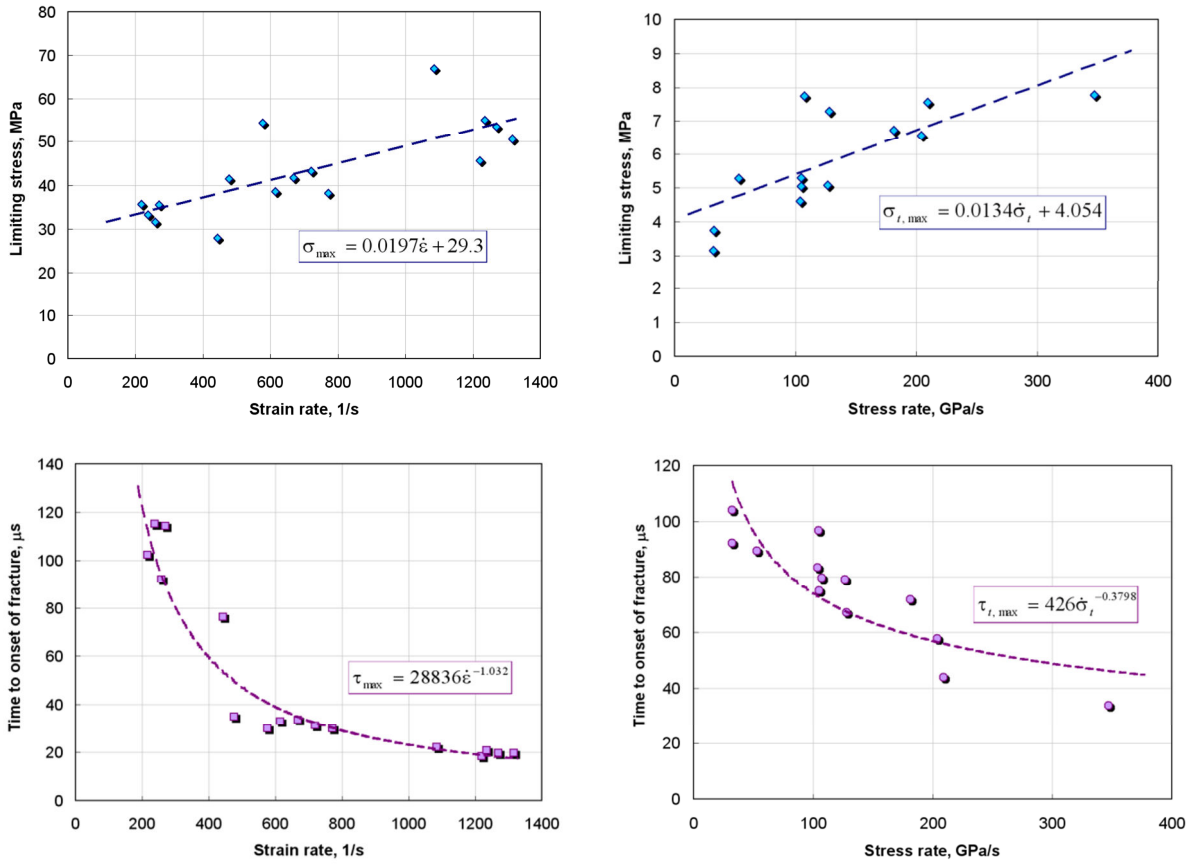

(a) (b)

Fig. 4 - Strength properties of ceramic brick in compression (a) and splitting (b)

The dependences of the ultimate strength characteristics of ceramic brick on the strain rate during compression and the rate of stress growth during splitting are plotted in Fig. 4.

Dynamic tests of fine-grained concrete M25 under compression were carried out on cylindrical specimens with a diameter of 20 mm and lengths of 20 and 10 mm in order to study the influence of the length of the specimens on the stress-strain curves of the material. In addition, to evaluate the effect of humidity on the material properties, samples with a diameter of 20 mm and a length of 10 mm were tested in a water-saturated state.

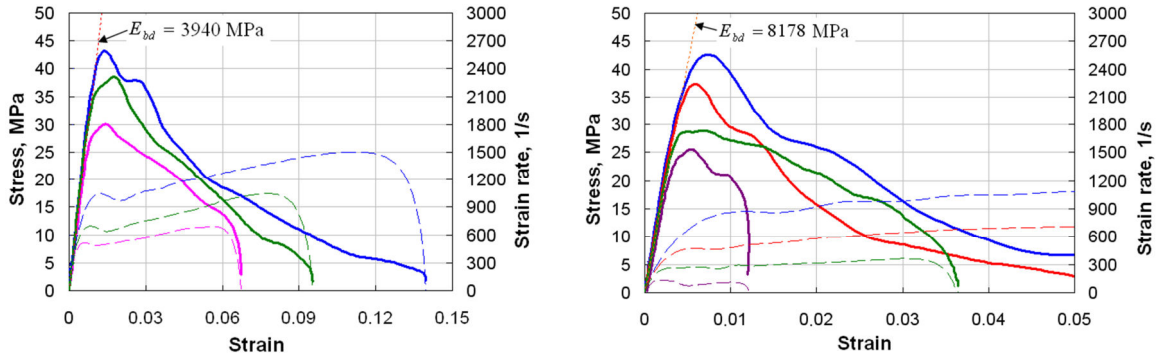

(a) (b)

Fig. 5 - Properties of fine-grained concrete in compression for specimen of length 10 mm (a) and 20 mm (b)

Figure 5 shows the average stress-strain curves under compression of fine-grained M25 concrete with the history of strain rate changes obtained for specimen length of 10 mm (a) and 20 mm (b). A well-known trend can be noticed: stress-strain curves of samples of longer length have greater steepness of the initial (elastic) section.

Further, the influence of the strength characteristics of fine-grained concrete of the geometry of the specimen (Fig. 6) and its moisture content is analyzed (Fig. 7).

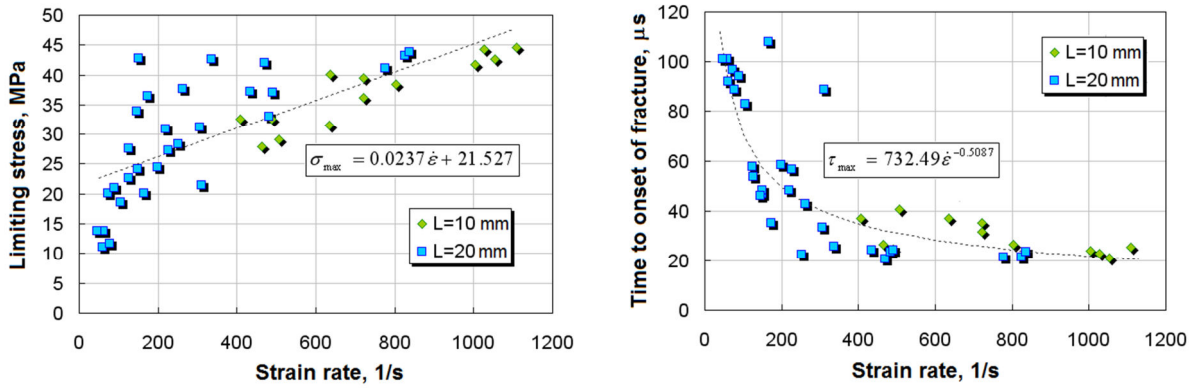

Fig. 6 - The influence of specimen geometry on compressive properties of fine-grade concrete M25

As a result of the static and dynamic experiments carried out, the dependence of the Dynamic Increase Factor (DIF) of concrete M25 on the strain rate (during compression tests) and on the rate of stress growth (under tension) was constructed. Assuming the behavior of the material before fracture to be elastic, in each test the strain rate was determined as $\dot{\varepsilon} = \dot{\sigma} / E$ (E=24 GPa - initial static modulus of elasticity of fine-grained M25 concrete).

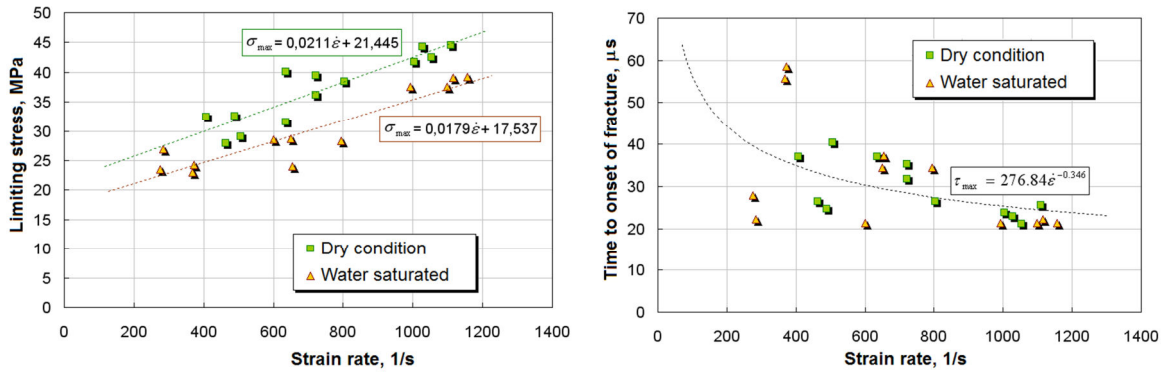

Fig. 7 - The influence of specimen humidity on compressive properties of fine-grade concrete M25 for specimen length of 20 mm

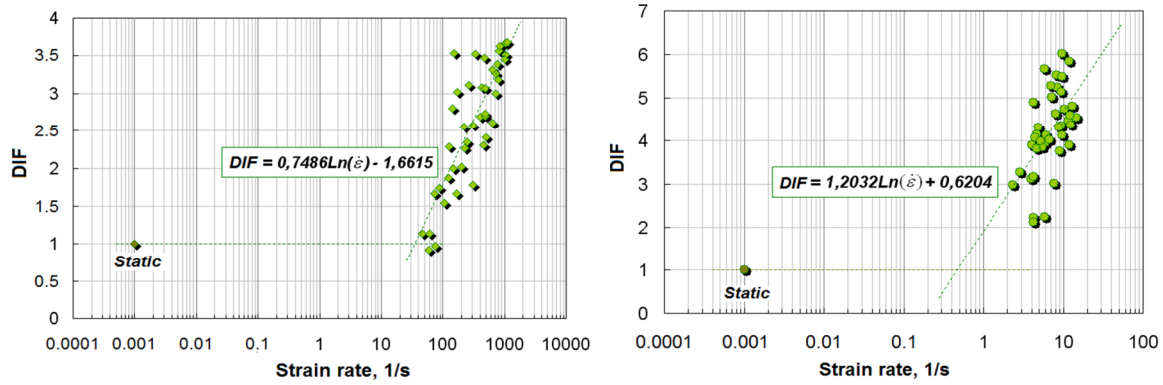

(a) (b)

Fig. 8 - The dynamic increase factor for fine-grade concrete B25 in compression (a) and splitting (b)

The dependences of the DIF on the strain rate for compression and splitting (Fig. 8) obtained for the investigated fine-grained concrete M25 are qualitatively and quantitatively in good agreement with the results of other studies of such concrete. DIF in the investigated range of strain rates reached four under compression and six under tension.

Dynamic tests of fine-grained fiber-reinforced concrete CARDIFRC were carried out by using the Kolsky technique for compression and splitting, shearing and three-point bending of beams weakened by a U-shaped notch.

Fig. 9 shows the obtained average stress-strain curves for fiber-concrete under compression (a) and splitting (b) at different strain rates.

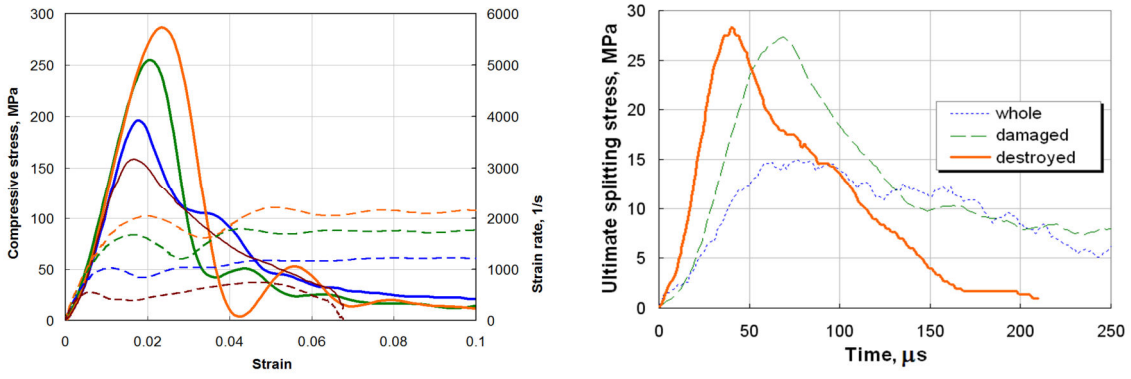

(a) (b)

Fig.9 Mechanical properties of fiber concrete in compression (a) and splitting (b)

Based on the obtained static and dynamic data, the dependences of the ultimate strength characteristics of fiber-reinforced concrete on the strain rate during compression and the rate of stress growth during splitting are plotted (Fig. 10).

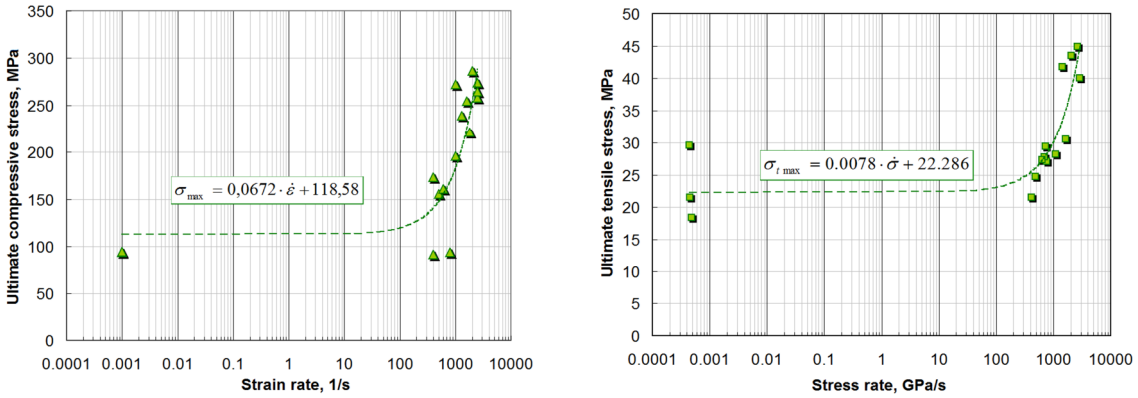

(a) (b)

Fig. 10 - Strength properties of fiber-reinforced concrete in compression (a) and splitting (b)

A series of experiments on shear was performed using the modified Kolsky method (Fig. 2). The average dependence of shear stress on time with confidence intervals at 95% reliability level is shown in Fig.11.

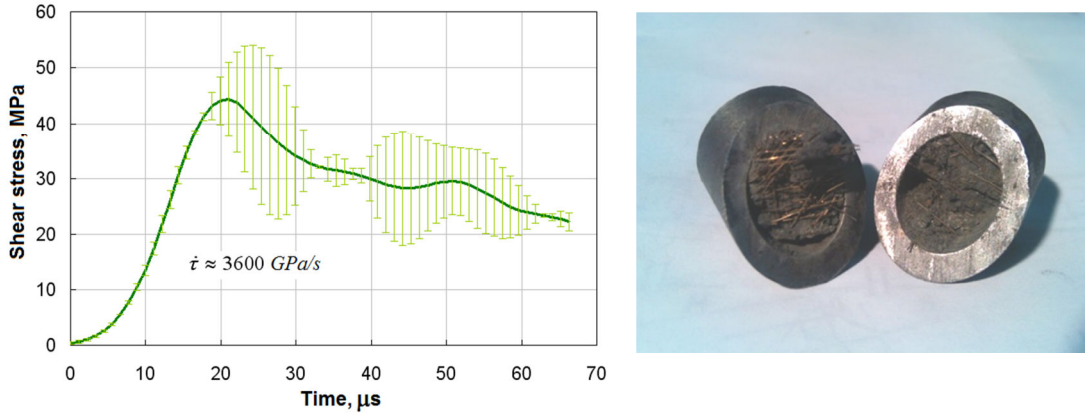

(a) (b)

Fig. 11 - The average dynamic chart obtained during the testing of fiber-reinforced concrete in shear (a) and the appearance of the specimen of the fiber-reinforced concrete after the test (b)

Tests of fiber-reinforced concrete for impact toughness were carried out in order to determine the critical load at which cracks in the sample form and begin to spread. In this connection, it was required to select a loading energy of the specimen at which a crack in the specimen was formed, but its complete failure did not occur. Tests of beams with different geometric dimensions were carried out on installations with different diameters of measuring bars to study the effect of the scale factor on the obtained values of impact toughness of fiber-reinforced concrete.

Due to the high brittleness of the matrix and low viscosity of the test material, micro-cracks were initiated at low amplitudes of loading pulses of different durations that can be realized at existing facilities. At larger amplitudes of the loading wave the specimen experienced significant deflections and it broke into two parts.

Since the contact area of the loading bar (wedge) and the sample is very small, most of the incident wave is reflected by the tensile wave and after reflection from the impacted end of the incident bar, the compression wave again reaches the specimen, loading it once more. This process is repeated many times with gradually decreasing amplitude. The deflection of the sample during one loading cycle is determined on the basis of the deformation pulses recorded in the measuring bars and is ~1 mm, whereas the actual deflection of the sample with a strongly opened crack after the test may reach ~17 mm. This is due to the multiple loading of the specimen with a gradually decreasing amplitude. Unfortunately, it is very difficult to record all loading cycles because of the insufficient length of the measuring bars.

Fig. 12a shows the values of the deflection of the sample as a function of the growth rate of the force on logarithmic scale of the rate of growth of forces for different durations of the loading pulse.

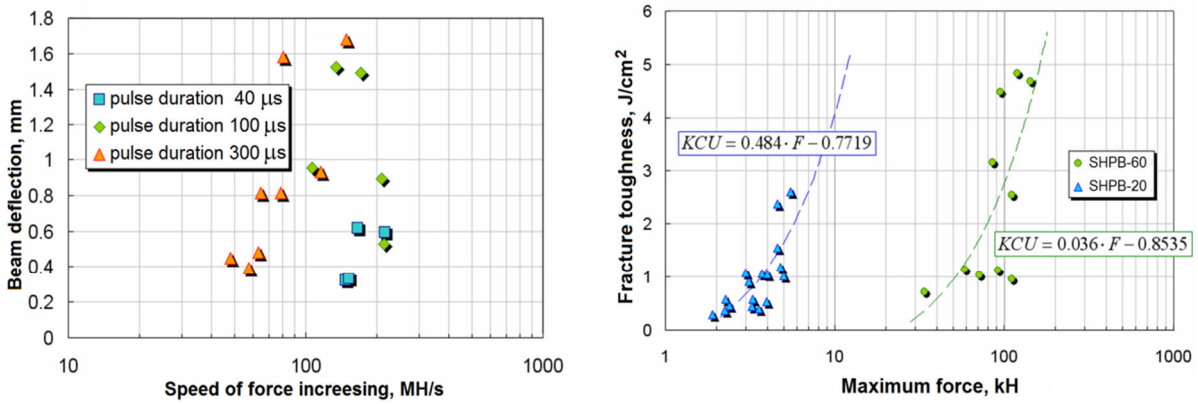

(a) (b)

Fig. 12 - Results of tests of fiber-reinforced concrete for fracture toughness

The values of the impact toughness as a function of the maximum force obtained in tests on the facilities with SHPB-20 and SHPB-60 are shown in Fig. 12b. This figure illustrates the effect of the scale factor on the fracture toughness for fiber-reinforced concrete. It can be seen that the failure of a large beam specimen with a U-shaped concentrator on the unit with SHPB-60 requires more energy per unit cross-sectional area of the sample at the site of the concentrator than the smaller sample on the unit with SHPB-20.

On the basis of the data obtained, it can be seen that as the magnitude and rate of growth of the applied load increase, the work expended during the loading cycle increases, and the work of impact, fracture toughness and deflection of the sample, depending on the maximum force, all vary nearly linearly. The work expended is almost the same for different durations of the loading pulse.

The dependences of strength characteristics on the rate of change of stress for the investigated fine-grained concretes obtained in the experiments can be calculated using the well-known criterion of incubation time (Petrov, Utkin, 1989; Petrov, Morozov, 1996). Fig. 13 shows the results of experiments and calculations by this criterion for fine-grained concrete M25, and Fig. 14 - for fine-grained fiber-concrete.

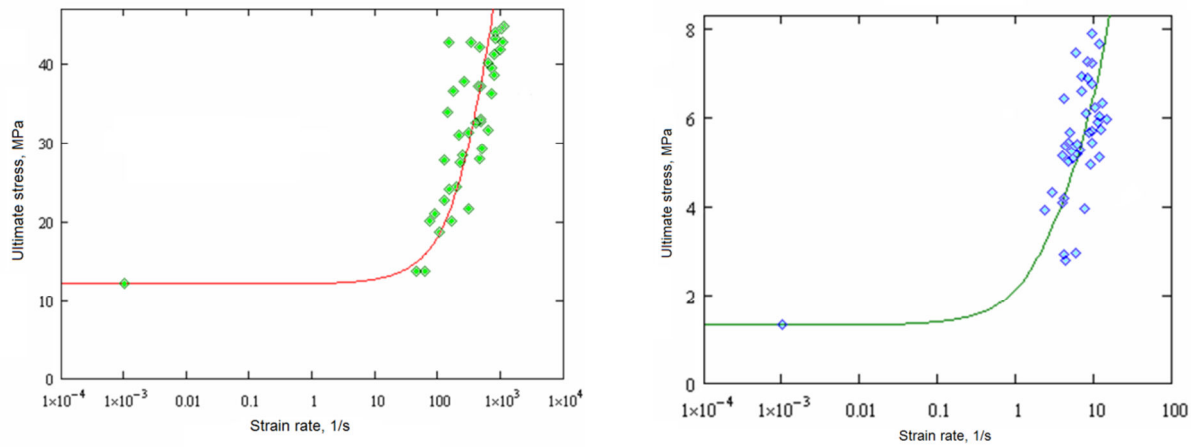

(a) (b)

Fig. 13 - Strength characteristics of fine-grained concrete M25, obtained in experiments (markers) and calculated by the criterion of incubation time (solid lines) under compression (a) and tension (b)

The calculation by the criterion of incubation time was performed at σ_{cr}^{comp} =12.1 MPa; E=24 GPa; τ=5 μs (a) and σ_{cr}^{tens} =1.31 MPa; E=24 GPa; τ=67 μs (b)

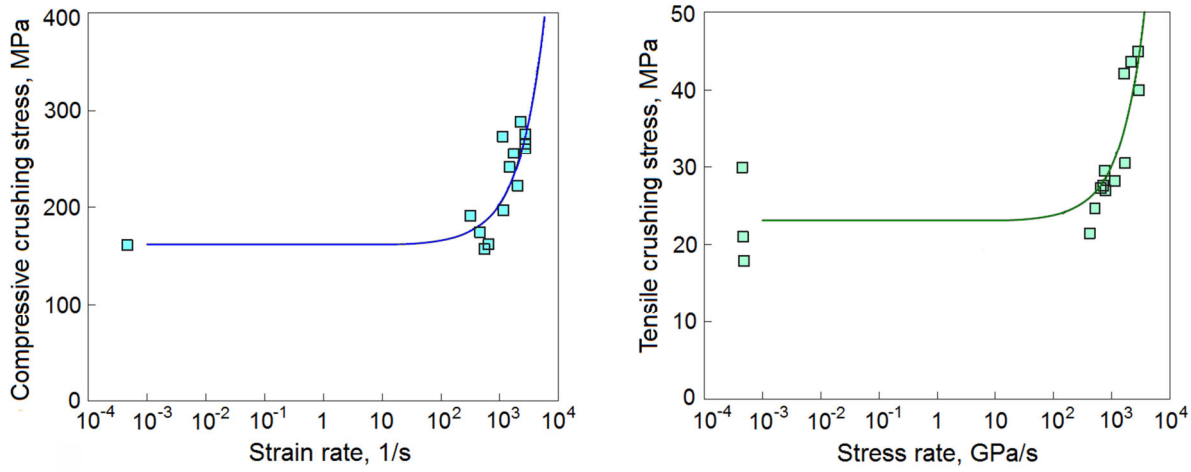

(a) (b)

Fig. 14 - Strength characteristics of fine-grained fiber-reinforced concrete CARDIFRC, obtained in experiments (markers) and calculated by the criterion of incubation time (solid lines) under compression (a) and tension (b)

The calculation by the criterion of incubation time was performed at σ_{cr}^{comp} =160 MPa; E=46 GPa; τ=2 μs (a) and σ_{cr}^{tens} =23 MPa; E=46 GPa; τ=15 μs (b)

Fig. 15 shows the dependence of the work of fracture on the rate of the specimen deflection during testing of three-point bend beams weakened by a U-shaped notch.

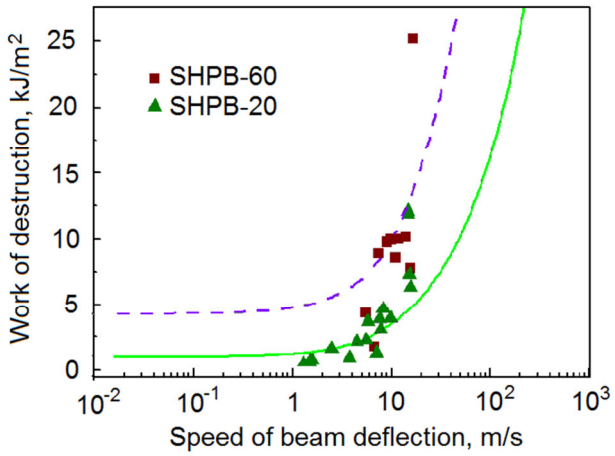

Fig. 15 - Energy characteristics of destruction of fiber concrete CARDIFRC, obtained in experiments (markers) and calculated by the criterion of incubation time (lines)

Calculation on the incubation time criterion for the three-point bending of a beam with a U-shaped concentrator was performed at τ=30 μs; W_c=4300 J/m^2; K=300 MN/m when tested at the SHPB-60 installation (dashed line) and at τ=30 μs; W_c=1000 J/m^2; K=18 MN/m for testing at the SHPB-20 installation (solid line).

From the results presented, it can be seen that the criterion of incubation time describes quite well the main experimental results obtained. Moreover, the value of the incubation time of fracture under tension was greater than in compression, and in the case of CARDIFRC fiber-reinforced concrete - of the same order as in the three-point bending of the beams.

CONCLUSION

Dynamic tests of brittle media under various stress-strain states have been carried out. The main attention was paid to the study of the change in the maximum stress and appropriate time before the onset of failure, depending on the strain rate or the rate of stress growth.

A comparison of the results of tests of fine-grained concrete and fiber-reinforced concrete showed that with an increase in the strain rate, an increase in strength is observed both in compression and in tension.

The obtained DIF dependences on the strain rate are qualitatively and quantitatively in good agreement with the known results of other researchers.

A unified interpretation of the velocity effects of the failure of the tested fine-grained concrete on the basis of the structural-temporal (incubation time based) approach is done. The values of the incubation time of destruction for different types of stress-strain state are determined that well describe the experimental data. It was noted that the value of the incubation time of fracture under tension was greater than in the case of compression for both concretes.

ACKNOWLEDGMENTS

The experimental investigations of bricks and fine-graned concrete were financed by RFBR (grants 15-08-05517, 16-01-00524 and 16-38-60122), determination of fiber concrete properties was done under financial support of the Russian Science Foundation (grant 16-19-10237). Y. Petrov was supported by the Russian Science Foundation (grant 17-11-01053).

REFERENCES

[1]-Alaee F.J., Karihaloo B.L., 2003 Retrofitting of RC beams with CARDIFRC: Journal of Composites for Construction (ASCE) 7(3), p.174-186.

[2]-Bragov A.M., Lomunov A.K., Konstantinov A.Yu., Lamzin D.A., 2017 A Modified Kolsky Method for Determining the Shear Strength of Brittle Materials. Technical Physics Letters, 43(1), p.85-87.

[3]-Petrov Y.V., Utkin A.A., 1989 Dependence of the dynamic strength on loading rate. Soviet Materials Science 25(2), p.153-156.

[4]-Petrov Y.V., 1991 On "Quantum" Nature of Dynamic Fracture of Brittle Solids. Dokl. Akad. Nauk USSR, 321 (1), p.66-68,

[5]-Petrov Y., Morozov N., 1994 On the modeling of fracture of brittle solids. ASME Journal of Applied Mechanics **61**, p.710-712.

[6]-Petrov Y.V., 2013 Structural-temporal approach to modeling of fracture dynamics in brittle media. In: Rock Dynamics and Applications - State of the Art /J.Zhao & J.Li (eds)/ Taylor & Francis Group, London. p.101-110.

[7]-Bragov A.M., Petrov Yu.V., Karihaloo B.L., Konstantinov A.Yu., Lamzin D.A., Lomunov A.K., Smirnov I.V., 2013 Dynamic strengths and toughness of an ultra high performance fibre reinforced concrete. Engineering Fracture Mechanics. 110, p.477-488.